Mesenchymal stem cells suppress leukemia via macrophage-mediated functional restoration of bone marrow microenvironment

Chengxiang Xia[1, 3, 4,7†], Tongjie Wang[1†], Hui Cheng[2,5†], Yong Dong[1, 3], Qitong Weng[1, 3], Guohuan Sun[2,5], Peiqing Zhou[1, 3], Kaitao Wang[6], Xiaofei Liu[1], Yang Geng[1], Shihui Ma[2,5], Sha Hao[2,5], Ling Xu[8], Yuxian Guan[1], Juan Du[1], Xin Du[9,10], Yangqiu Li[8], Xiaofan Zhu[2,5], Yufang Shi[11], Sheng Xu[12], Demin Wang[13,14], Tao Cheng[2,5*], Jinyong Wang[1, 3, 4, 6, 7*]

[1]State Key Laboratory of Experimental Hematology, CAS Key Laboratory of Regenerative Biology, Guangzhou Institutes of Biomedicine and Health, Chinese Academy of Sciences, Guangzhou, China; [2]State Key Laboratory of Experimental Hematology & National Clinical Research Center for Blood Diseases, Institute of Hematology & Blood Diseases Hospital, Chinese Academy of Medical Sciences & Peking Union Medical College, Tianjin, China; [3]Guangzhou Regenerative Medicine and Health-Guangdong Laboratory (GRMH-GDL), Guangzhou, China; [4]Guangdong Provincial Key Laboratory of Stem cell and Regenerative Medicine, Guangzhou Institutes of Biomedicine and Health, Chinese Academy of Sciences, Guangzhou, China; [5]Center for Stem Cell Medicine & Department of Stem Cell and Regenerative Medicine, Chinese Academy of Medical Sciences & Peking Union Medical College, Tianjin, China; [6]Joint School of Life Sciences, Guangzhou Institutes of Biomedicine and Health, Guangzhou Medical University, Guangzhou, China; [7]University of Chinese Academy of Sciences, Beijing, China; [8]Department of Hematology, First Affiliated Hospital; Institute of Hematology, School of Medicine; Key Laboratory for Regenerative Medicine of Ministry of Education; Jinan University, Guangzhou, China; [9]Department of Hematology, Guangdong Provincial People's Hospital (Guangdong Academy of Medical Sciences), Guangzhou, Guangdong, China; [10]South China University of Technology, Guangzhou, China; [11]The First Affiliated Hospital of Soochow University, State Key Laboratory of Radiation Medicine and Protection, Institutes for Translational Medicine, Soochow University, Suzhou, China; [12]National Key Laboratory of Medical Immunology & Institute of Immunology, Second Military Medical University, Shanghai, China; [13]Blood Research Institute, Versiti, Milwaukee, WI, USA; [14]Biomedical Research Center of South China, College of Life Sciences, Fujian Normal University, Fuzhou, China.

[†]Equal contributors.

[*]Correspondences:

Jinyong Wang (J.W.), E-mail: wang_jinyong@gibh.ac.cn

Tao Cheng (T.C.), E-mail: chengtao@ihcams.ac.cn

33 **Key Points:**

34 *Key Point 1*: Intra-BM transfusion of MSCs restores the BM microenvironment, improves
35 thrombopoiesis, and suppresses MDS/MPN initiated by *Nras* mutation.

36 *Key Point 2*: Donor MSCs reprogram macrophages to restore the BM microenvironment, improve
37 thrombopoiesis, and suppress leukemia.

Abstract

Bone marrow (BM) mesenchymal stem cells (MSCs) are critical components of the BM microenvironment and play an essential role in supporting hematopoiesis. Dysfunction of MSCs is associated with the impaired BM microenvironment that promotes leukemia development. However, whether and how restoration of the impaired BM microenvironment can inhibit leukemia development remain unknown. Using an established leukemia model and the RNA-seq analysis, we discovered functional degeneration of MSCs during leukemia progression. Importantly, intra-BM instead of systemic transfusion of donor healthy MSCs restored the BM microenvironment, thus systemically altering cytokine expression patterns, improving normal hematopoiesis, reducing tumor burden, and ultimately prolonging survival of the leukemia-bearing mice. Donor MSC treatment restored the function of host MSCs and reprogrammed host macrophages to fulfill tissue-repair function. Transfusion of MSC-reprogrammed macrophages largely recapitulated the therapeutic effects of MSCs. Further, we found that donor MSCs reprogrammed macrophages to reduce leukemia burden through autocrine of IL-6. Taken together, our study reveals that donor MSCs reprogram host macrophages to restore the BM microenvironment and inhibit leukemia development, thus offering rationales for local MSC administration as a potentially effective therapy for leukemia.

55 **Introduction**

56 BM MSCs are key components of the BM stromal microenvironment, regulating homeostasis of
57 the stromal niche and hematopoiesis[1]. Accumulating evidence uncovers that dysfunction of MSCs
58 is associated with leukemia progression. Leukemic MSCs in a mouse T-ALL model suppressed
59 normal hematopoiesis[2]. Deletion of *Dicer1* gene in MSCs leads to impaired osteogenic
60 differentiation, thrombopenia, and secondary tumorigenesis[3]. In myeloproliferative neoplasms, the
61 leukemic cells reprogram MSCs to support proliferation of leukemic stem cells[4]. Ablation of MSC-
62 derived osteoblasts impairs the homeostasis of hematopoietic stem cells (HSC) and accelerates
63 leukemogenesis in chronic myeloid leukemia[5]. In a myelodysplastic/myeloproliferative neoplasms
64 (MDS/MPN) model, *Ptpn11* mutation in MSCs hyperactivates HSC by secreting CCL3,
65 systemically resulting in myeloid-biased proliferation and promoting leukemia progression[6].
66 Chromosomal abnormalities in MSCs occur in over 16% MDS/acute myeloid leukemia (AML)
67 patients, which leads to a shorter survival[7]. MSCs of every MDS patient show features of stemness
68 loss, aging, and osteogenic differentiation defect, which results in insufficient hematopoiesis[8]. In
69 a patient-derived xenograft (PDX) model, only co-transplantation of tumor cells and the same
70 patient-derived MSCs successfully recapitulates the MDS phenotype, indicating that besides the
71 loss of function of supporting hematopoiesis, MSCs in MDS patients may acquire a function of
72 preferentially promoting tumorigenesis[9]. Despite these findings, the causal relationship between
73 tumor cells and the BM microenvironment during leukemia development and progression remains
74 elusive.

75 MSC therapy has been widely used in treating immune-related graft-vs-host disease (GVHD) and
76 inflammation-related diseases[10,11]. Over the decades, a lot of evidence demonstrates that MSCs
77 regulate innate and adaptive immune responses largely by secreting distinct sets of cytokines,

78 growth factors, and chemokines depending on different disease contexts[12-16]. Given the short
79 lifespan of donor MSCs after transfusion[17], the underlying molecular and cellular mechanisms by
80 which these cells produce therapeutic effects remain elusive. It is also completely unknown
81 whether donor MSCs can restore the impaired BM microenvironment and consequently suppress
82 disease progression in leukemia setting.
83 Macrophages are pivotal for maintenance of the tissue microenvironment, tissue repair, and even
84 the tumor microenvironment[18-22]. BM resident macrophages maintain the homeostasis of HSCs
85 and loss of these macrophages leads to mobilization of HSCs into peripheral blood (PB)[23]. The
86 functions of macrophages are plastic and can be reshaped by distinct sets of soluble factors. When
87 performing tissue repair, macrophages highly express arginase 1 (*Arg1*)[24], an enzyme that converts
88 L-arginine to urea and L-ornithine. After co-culture with MSCs, macrophages can be polarized
89 from pro-inflammation (M1) to anti-inflammation (M2) type, up-regulating IL-10 and CD206 and
90 down-regulating IL-6 and IL-1β[25]. Upon stimulated by LPS or TNF-α, MSCs can cross-talk with
91 lung macrophages and reprogram these macrophages to secrete IL-10 to alleviate sepsis[26]. Despite
92 these knowledge, whether healthy MSCs can reprogram macrophages from leukemia-bearing host
93 to repair the damaged BM microenvironment is not known.
94 Using the established mouse model mimicking chronic MPN/MDS diseases[27-29], we discovered
95 that the deteriorating BM microenvironment was associated with disease progression. Intra-BM
96 instead of systemic transfusion of healthy MSCs restored the local BM microenvironment,
97 improved thrombopoiesis, reduced tumor burden, and prolonged survival of leukemia-bearing
98 mice. Mechanistically, we found that MSCs suppress leukemia development through resident
99 macrophages and autocrine effect of IL-6. Our study demonstrates that intra-BM transfusion of

100 MSCs can restore the local BM niche to systemically prevent leukemia progression and can be a
101 novel therapy for leukemia.

102 **Materials and Methods**

103 **Mice.** All mouse strains were maintained on C57BL/6 genetic background. Mice expressing the
104 conditional oncogenic NrasG12D mutation (a gift from Dr. Jing Zhang lab at University of
105 Wisconsin-Madison, Wisconsin, USA) were crossed to Vav-Cre mice to generate *LSL Nras*/+;
106 *Vav-Cre* compound mice (NV mice). Genotyping of the adult mice was performed as described
107 previously[27]. Vav-Cre strain (CD45.2), wild-type CD45.2, CD45.1 strain (C57BL/6) and *Il6* knock
108 out strain (*Il6*$^{-/-}$, C57BL/6) were purchased from Jackson lab. GFP strain (CD45.2) was gifted by
109 Guangdong Laboratory Animals Monitoring Institute. *MLL-AF9* AML model mice were
110 maintained a specific pathogen-free animal facility at the State Key Laboratory of Experimental
111 Hematology. All mice were maintained within the SPF grade animal facility of Guangzhou
112 Institution of Biomedicine and Health, Chinese Academy of Science (GIBH, CAS, China). All
113 animal experiments were approved by the Institutional Animal Care and Use Committee of
114 Guangzhou Institutes of Biomedicine and Health (IACUC-GIBH).

115 **NrasG12D leukemia model.** White blood cells (CD45.2^{+}, 0.3 million) after depletion of stromal
116 cells from NrasG12D compound mice (*LSL Nras/+; Vav-Cre*) or control mice (CD45.2 strain)
117 were sorted and transplanted into sublethally (6.5 Gy, RS2000, Rad Source Inc) irradiated CD45.1
118 recipient by retro-orbital intravenous injection. Mice were fed with trimethoprim-
119 sulfamethoxazole-treated water for two weeks to prevent infection. Hematopoietic lineages in PB
120 were assessed monthly by flow cytometry. During the development of NrasG12D-induced
121 leukemia, the CD11b^{+} percentage in PB indicated the tumor burden (CD11b^{+}%).

122 **RNA-Seq and data analysis.** For MSC library preparation, MSCs were sorted from wild type or
123 leukemia-bearing mice, and recovered MSCs were sorted from leukemia-bearing mice 8 weeks
124 post treatment with GFP^+ donor MSCs. MSCs were sorted from two mice of each group. 1000
125 target cells per sample were sorted into 500 µl DPBS-BSA buffer (0.5%BSA) using 1.5ml EP tube
126 and transferred into 250 µl tube to spin down with 500 g. The cDNA of sorted 1000-cell aliquots
127 were generated and amplified as described previously[30]. The qualities of the amplified cDNA were
128 examined by Q-PCR analysis of housekeeping genes (*B2m, Actb, Gapdh, Ecf1a1*). Samples passed
129 quality control were used for sequencing library preparation by illumina Nextera XT DNA Sample
130 Preparation Kit (FC-131-1096).
131 For macrophages (*in vivo*) library preparation, macrophages were sorted from BM of leukemia-
132 bearing mice before or after MSC treatment (12 hours post MSC treatment). Macrophages were
133 also sorted after 12 hours of co-culture with MSCs. 1 × 10^5 target cells per sample were sorted
134 and total RNA was extracted using the RNeasy micro kit with on-column DNase treatment
135 (Qiagen, 74004) according to manufacture's protocol. cDNA library was constructed using
136 VAHTSTM mRNA-seq V3 Library Prep Kit for Illumina (Vazyme, NR611) according to
137 manufacture's protocol. The qualities of the cDNA were examined by qPCR analysis of
138 housekeeping genes (*B2m, Actb, Gapdh, Ecf1a1*). Samples that passed quality control were used
139 for sequencing.
140 For data analysis, all libraries were sequenced by illumina sequencers NextSeq 500. The fastq files
141 of sequencing raw data samples were generated using illumina bcl2fastq software (version:
142 2.16.0.10) and were uploaded to Gene Expression Omnibus public database (GSE 125029). Raw
143 reads were aligned to mouse genome (mm10) by HISAT2[31] (version: 2.1.0) as reported. And raw
144 counts were calculated by featureCounts of subread[32] (version 1.6.0). Differential gene expression

145 analysis was performed by DESeq2[33] (R package version: 1.18.1). Unsupervised clustering
146 analysis was performed using facotextra (R package, version：1.0.5). Heatmaps were plotted
147 using gplots (R package, version 3.01). GSEA was performed as described[34], and gene-ontology
148 (GO)-enrichment analysis were performed by clusterProfiler[35] (R package, version: 3.6.0). MSC
149 stemness related genes and MSC osteogenesis related genes for heatmaps were from references as
150 follows: MSC stemness-related genes[36-38] and MSC osteogenesis-related genes[36,39]. The gene sets
151 for GSEA were from literatures as follows: angiogenesis-related genes in macrophages[40], cell
152 migration-related genes in macrophages (from MSigDB genesets), and secreted factors by
153 macrophages[41,42].

154 **MSC treatment for leukemia-bearing mice.** For MSC transfusion, multiple approaches
155 including retro-orbital, tail intravenous, and local intra-BM transfusion were applied
156 independently. For tail vein transfusion, each leukemia-bearing mouse was injected with 2.5 ×
157 10^7 MSCs/kg (Passage 2) in 100 μl DPBS by tail vein transfusion. For retro-orbital transfusion,
158 each leukemia-bearing mouse was injected with 2.5 × 10^7 MSCs/kg (Passage 2) in 200 μl DPBS
159 by retro-orbital transfusion. For local intra-BM transfusion, tibia of each leukemia-bearing mouse
160 was injected with 2.5 × 10^7 MSCs/kg (Passage 2) in 20 μl DPBS by local intra-BM transfusion.
161 MSCs were injected once every two weeks and continued in a time window of 16 weeks. Every
162 tibia was treated once per month by switching the injection site every other dose. The control mice
163 were injected with DPBS following the same treatment procedure as MSCs. Analysis of platelets
164 and $CD11b^+$ cells in PB was performed monthly.

165 **GFP-MSCs and BM macrophage co-culture assay.** Short-term co-culture assay was performed,
166 with each well containing: 1 × 10^5 GFP-MSCs (passage 2; healthy MSCs were isolated from
167 GFP mice, *Il6*$^{-/-}$ MSCs were isolated from *Il6*$^{-/-}$ mice) and 2 × 10^6 $CD11b^+$ leukemic cells sorted

168 from leukemia-bearing mice in 2 mL culture medium of α-MEM, 10% FBS and 50 ng/ml SCF.
169 MSCs and $CD11b^+$ leukemic cells were incubated either by direct-contact culture or transwell
170 culture for 12 hours at 37^oC under 5% CO_2 in a humidified incubator. MSC-reprogrammed
171 macrophages from leukemia-bearing mice ($CD11b^+F4/80^+$) were sorted for detecting the gene
172 expression by Q-PCR.

173 **Treatment for leukemia-bearing mice with MSC-reprogrammed macrophages.** 1 × 10^5
174 MSCs were seeded into each well of six-well plates. $CD11b^+$ leukemic cells were enriched from
175 BM of leukemia-bearing mice with severe tumor burden ($CD11b^+$% in PB > 60%). Then 2 × 10^6
176 $CD11b^+$ leukemic cells were directly co-cultured with MSCs. After 12 hours, macrophages were
177 sorted for transfusion. Leukemia-bearing mice with severe tumor burden were treated by intra-BM
178 transfusion of PBS or MSC-reprogrammed macrophages from leukemia-bearing mice (E-Mac). A
179 dose of 1 million macrophages/mouse in 20 μl PBS were delivered into the tibia cavity using 29-
180 gauge needle. Every tibia was treated once per two weeks by switching the injection site every
181 other dose. Analysis of platelets and $CD11b^+$ cells in PB was performed monthly.

182 **Statistical analysis.** The data were represented as mean ± SD. Two-tailed independent Student's
183 t-tests were performed for comparison of two groups of data (SPSS v.23, IBM Corp., Armonk,
184 NY, USA). For the analysis of three groups or more, one-way ANOVA was used (SPSS v.23, IBM
185 Corp., Armonk, NY, USA), and further significance analysis among groups was analyzed by Post
186 Hoc Test (equal variances, Turkey-HSD; unequal variances, Games-Howell). Kaplan-Meier
187 method was used to calculate survival curves of leukemia, and Log-rank (Mantel-Cox) test was
188 performed to compare differential significance in survival rates. P values of less than 0.05 were
189 considered statistically significant (*$p < 0.05$, **$p < 0.01$, ***$p < 0.001$).

190 **Results**

191 **Deterioration of BM MSCs accompanies the development of *Nras*-mutant-induced leukemia**

192 Mice carrying an endogenous mutant *Nras* allele develop myelodysplastic/myeloproliferative
193 neoplasms (MDS/MPN)-like leukemia with a long latency[27-29,43]. Here we found the primary BM
194 leukemic cells failed to accelerate the disease in the secondary recipient mice, implying a role of
195 the BM microenvironment in disease etiology (Figure S1). We hypothesized that the BM
196 microenvironment is impaired by *Nras*-mutant leukemic cells, which in return impedes normal
197 hematopoiesis and accelerates leukemia progression. Indeed, we observed quantitative decreases
198 and functional degeneration of MSCs ($Ter119^-CD45^-CD31^-Sca1^+CD51^+CD146^+$) during disease
199 development and progression (Figure 1A-C, and Figure S2). To further characterize the residual
200 MSCs in mice with leukemia, we performed RNA-Seq analysis of the residual MSCs from
201 leukemia-bearing mice at an early disease phase ($CD11b^+$% in PB: 35%-45%). Consistent with
202 the quantitative and functional reduction, the expression of the transcription factor *Gnl3*[36], an
203 indicator of MSC self-renewal, was significantly down-regulated in MSCs from leukemia-bearing
204 mice relative to wild-type mice (Figure 1D). The expression of *Nt5e* (CD73), *Thy1* (CD90), *Vcam1*
205 (CD106), *Cd81*, *Sdc4*, *Itgb1* and *Anpep*[36-38], encoding surface markers on three-lineage-potent
206 MSCs but not on uni-lineage-primed MSCs, was markedly reduced in MSCs from leukemia-
207 bearing mice (padj < 0.05, fold change > 1.6) (Figure 1D). Furthermore, the expression of *Bgn*,
208 *Bmp4*, *Col1a1*, *Csf1*, *Dcn*, *Dkk2*, *Mmp13*, *Ogn*, *Wisp1*, and *Wisp2*[36,39], pivotal for osteogenic
209 differentiation, was markedly suppressed in the residual MSCs (padj < 0.05, fold change > 2)
210 (Figure 1E). *In vitro* differentiation assay confirmed that osteogenic and adipogenic differentiation
211 potential in leukemic MSCs were impeded (Figure S3). MSCs fulfill their tissue-specific and
212 condition-responsive regulatory functions through secreting distinct types of soluble factors[44].
213 Under leukemia condition, the residual MSCs indeed secreted much less soluble factors, including

214 *Il6, Il11, Ccl2, Ccl7, Cxcl12, Cxcl13* and *Cxcl14* (padj < 0.05, fold change > 2), compared to MSCs
215 from normal wild-type mice (Figure 1F). These molecules are pivotal for tissue repairing[45-50].
216 Indirect immunofluorescence assay and intracellular flow cytometry staining confirmed that the
217 levels of IL-6 (Figure 1G-H), CCL2 (Figure 1I-J), and CXCL12 (Figure 1K-L) proteins in
218 leukemic MSCs were significantly lower than healthy MSCs ($p < 0.001$). In addition, *Ccl5,* a
219 chemokine involved in the pathogenesis of MPN[51] and the inhibition of thrombopoiesis[52], was
220 significantly up-regulated in the residual MSCs from leukemia-bearing mice (padj < 0.05, fold
221 change > 2). Gene set enrichment analysis (GSEA) further revealed features of inflammation in
222 the residual MSCs (Figure S4). Collectively, these results show that the MSCs dramatically
223 deteriorate during the disease development and progression of *Nras*-mutation-caused leukemia.

224 **Intra-BM transfusion of healthy MSCs improves thrombopoiesis, reduces tumor burden and**
225 **improves survival of the leukemia-bearing mice**

226 We hypothesized that restoration of the impaired BM microenvironment in leukemia-bearing mice
227 might suppress/delay the disease progression. To test this hypothesis, we attempted healthy MSC
228 treatment using GFP-tagged MSCs isolated from the tibias and femurs of healthy mice as
229 previously reported[53]. The isolated primary MSCs were expanded shortly *in vitro* to passage two
230 (P2) and cryopreserved. For MSC treatment, the cryopreserved P2 MSCs were recovered and
231 cultured for five days, phenotypically identified ($CD45^-Ter119^-CD31^-$
232 $CD51^+CD105^+LepR^+PDGFR\alpha^+PDGFR\beta^+Sca1^+$) (Figure S5), and suspended in DPBS (2.5 ×
233 10^7/ml) for transfusion. Initially, we adopted a direct delivery procedure by injecting donor
234 MSCs every two weeks either via tail vein (dose: 0.5 × 10^6/mouse) (Figure S6A) or retro-orbital
235 (dose: 0.5 × 10^6/mouse) transfusion (Figure S6B) into the leukemia-bearing mice at a late disease
236 phase ($CD11b^+$ cells > 60% in PB). However, these delivery approaches failed to produce

237 therapeutic effects. *In vitro* cultured MSCs lose their natural homing feature[54], the retro-orbital and
238 intravenous injection of cultured MSCs failed to home to bone marrow (Figure S6C-D). Thus, we
239 attempted intra-BM transfusion to overcome the homing defect caused by *in vitro* culture. A
240 sequential doses of MSCs (2.5 × 10^7 MSCs/kg per dose in 20 μL DPBS) were injected into the
241 tibia cavities of leukemia-bearing mice with two-week intervals for up to 16 weeks (Figure 2A).
242 Strikingly, the tumor burden continuously decreased during MSC treatment (Figure 2B and
243 Supplementary Figure S7). Consequently, the survival of treated leukemia-bearing mice was
244 significantly prolonged (Untreated: 51.5 days, MSC-treated: >115 days, $p < 0.001$) (Figure 2C).
245 Therefore, intra-BM transfusion of healthy donor MSCs improves the survival of leukemia-
246 bearing mice.

247 **MSC-treatment systemically re-balances myelopoiesis and activates megakaryopoiesis**

248 We next investigated the underlying mechanisms associated with the systemically decreased tumor
249 burden. We found that the hematopoiesis in the MSC-treated leukemia-bearing mice was re-
250 balanced, demonstrated by significant decreases of white blood cells (Untreated vs. MSC-treated:
251 23.04 vs 8.876, $p = 0.009$), and significant elevation of platelets (Untreated vs. MSC-treated: 2.64
252 vs. 6.01, $p = 0.004$) (Figure 2D) in PB. On the contrary, the PBS-treated leukemia-bearing mice
253 exhibited neither improved hematopoiesis (Figure S8) nor prolonged survival. High GM-CSF
254 levels in serum are associated with the tumor burdens of CMML in patients[55] and mouse models[27].
255 We analyzed the GM-CSF levels in serum of leukemia-bearing mice with or without MSC-
256 treatment. As expected, the GM-CSF levels in MSC-treated leukemia-bearing mice were
257 significantly decreased (> 7 folds) ($p < 0.001$) (Figure 2E), which was associated with the reduction
258 of GM-CSF secreting tumor cells (Figure S9). IL-6 promotes thrombopoiesis by increasing
259 systemic TPO levels[56]. Consistently, the MSC-treated leukemia-bearing mice exhibited elevated

260 IL-6 (> 25 folds) and TPO (> 2 folds) levels (Figure 2F) in PB serum. Collectively, these results
261 indicate that intra-BM transfusion of healthy donor MSCs systemically improves hematopoiesis
262 and prolongs the survival of leukemia-bearing mice.
263 To further investigate the systemic effects of the local MSC-treatment on hematopoiesis in
264 leukemia-bearing mice, we analyzed the ratios of myeloid progenitor subpopulations in MSC-
265 treated leukemia-bearing mice. Consistent with the elevated platelet levels and reduced myeloid
266 cells in PB, the MSC-treated leukemia-bearing mice showed increased proportions of
267 megakaryocyte-erythroid progenitors (MEP) (> 1.6 folds) ($p < 0.001$) and decreased ratios of
268 granulocyte-macrophage progenitors (GMP) (> 1.5 folds) ($p < 0.001$) in both injected and non-
269 injected sites than those sites in PBS-treated leukemia-bearing mice (Figure 3A-B, Figure S10A).
270 In addition, we observed increased (> 1.3 folds) ratios of mature megakaryocytes (≥ 8N) in both
271 injected and non-injected sites in MSC-treated leukemia-bearing mice (Figure 3C-D, Figure S10B)
272 in comparison with PBS-treated leukemia-bearing control mice ($p < 0.001$). Thus, these data
273 demonstrate that MSC-treatment systemically re-balances myelopoiesis and activates
274 megakaryopoiesis in leukemia-bearing mice.
275 **Recovered host MSCs are functional as healthy counterparts**
276 Consistent with an early report[57], our data showed that MSCs indeed support normal
277 hematopoiesis. Interestingly, MSCs also promoted the growth of leukemic cells *in vitro*, which
278 suggests that donor MSCs indirectly inhibit the tumor development *in vivo*. To investigate whether
279 the improved hematopoiesis is associated with restoration of the BM microenvironment, we
280 analyzed the MSC-treated tibias eight weeks after MSC treatment. Interestingly, host MSCs (GFP
281 negative) were partially recovered (Figure 4A-B), but restricted to the locally treated tibias (Figure
282 S11). Functionally, the recovered host MSCs formed markedly more CFU-F colonies than the

283 residual MSCs from untreated leukemia-bearing mice (> 3.8 folds) ($p < 0.001$) (Figure 4C and
284 Figure S12). To characterize the recovered MSCs at the transcriptome level, we sorted the
285 recovered MSCs for RNA-Seq analysis. Unsupervised hierarchical clustering analysis showed that
286 the recovered MSCs clustered closer to healthy MSCs (Figure 4D). Further, the expression of
287 cytokines and chemokines, including *Il6*, *Ccl2, Ccl7, Ccl19, Cxcl12, Cxcl13,* and *Cxcl14*, was
288 restored in the recovered MSCs compared to that in MSCs from untreated leukemia-bearing
289 control mice (padj < 0.05, fold change > 2) ($p < 0.05$) (Figure 4E). Consistently, indirect
290 immunofluorescence assay and intracellular flow cytometry staining confirmed that the levels of
291 IL-6, CCL2, and CXCL12 proteins in recovered MSCs (from the injected sites) were significantly
292 improved to comparable levels as in healthy MSCs ($p < 0.001$) (Figure 4F-I and S13). Therefore,
293 donor MSC-treatment results in local functional restoration of host MSCs.

294 **The donor MSCs reprogram macrophages to execute tissue-repair function**

295 We further investigated the cellular mechanism underlying the restored BM microenvironment
296 mediated by donor MSCs under leukemia condition. BM macrophages play a pivotal role in
297 maintaining the BM niche[18]. To study whether donor MSCs reprogram BM macrophages, we
298 performed co-culture assay of healthy MSCs with BM macrophages (L-Mac) sorted from the
299 leukemia-bearing mice *in vitro* for twelve hours and re-sorted the macrophages (E-Mac) for RNA-
300 Seq analysis. GSEA illustrated that angiogenesis-related genes, including *Vegfa, Hif1a, Serpine1,*
301 *Eng and Thbs1*[40] (Figure S14A), were enriched among the differentially expressed genes in E-Mac
302 (Figure 5A). Genes associated with cell migration, including *Sirpa* and *Ccl5*[58,59], were also
303 enriched in E-Mac (Figure 5B and S14B). Further, gene-ontology analysis demonstrated features
304 of positive regulation of cell migration and angiogenesis in E-Mac (Figure 5C). Elevated
305 expression of genes encoding soluble factors, including *Tnf*, *Il1a*, *Ccr7*, *Ccl3*, and *Ccl5*, was also

306 observed in E-Mac (Figure 5D). Indirect immunofluorescence assay confirmed that E-Mac had
307 significantly higher levels of TNF-α, CCR7, and IL-1α proteins than L-Mac ($p < 0.001$) (Figure
308 5E and S15A). Furthermore, intracellular flow cytometry staining also showed that the levels of
309 TNF-α and CCR7 proteins in L-Mac were significantly lower than E-Mac ($p < 0.001$) (Figure
310 S15B-D). To characterize which subset of macrophages are involved in re-educating the bone
311 marrow microenvironment, we analyzed the classical M1 and M2 macrophage subtypes both *in*
312 *vitro* and *in vivo*. However, the results showed that MSC treatment caused no typical transition of
313 M1 and M2 (Figure S16), which indicates a functional alteration of leukemic macrophages
314 independent of M1 to M2 transition. RNA-Seq analysis showed that the expression of arginase 1
315 (*Arg1*), an indicator of tissue repair function[24], was dramatically up-regulated over thousand folds
316 in E-Mac (Figure 5F) after direct co-culture with MSCs *in vitro*. However, the *Arg1* expression in
317 macrophages after transwell co-culture was barely elevated (Figure 5F), indicating that direct cell-
318 cell interaction instead of MSC-secreted soluble factors is essential for the functional
319 reprogramming. Consistent with the observation *in vitro*, the expression of *Arg1* was also
320 significantly increased in BM macrophages directly isolated from MSC-treated leukemia-bearing
321 mice (Figure 5G). Furthermore, intracellular flow cytometry staining confirmed that the ratios of
322 $Arg1^{high}$ macrophage subpopulation significantly increased in E-Mac at the MSC-treated sites (p
323 < 0.01) (Figure 5H-I). Collectively, these results indicate that the donor MSCs reprogram BM
324 macrophages from leukemia-bearing mice to execute tissue-repair function.

325 **The E-Mac treatment largely recapitulates the therapeutic effects of MSC treatment**

326 Given the short lifespan of donor MSCs *in vivo*[17], we speculated that MSCs mediate the restoration
327 of the BM microenvironment of leukemia-bearing mice by reprogramming macrophages. We
328 isolated macrophages from leukemia-bearing mice and co-cultured them with healthy MSCs for

329 12h, and then transplanted these E-Mac back into leukemia-bearing mice by intra-BM injection
330 (Figure 6A). We indeed found that the thrombopoiesis was significantly improved (> 6 folds) after
331 E-Mac treatment ($p < 0.001$) (Figure 6B-C). Host MSCs were also significantly increased (> 3
332 folds) in E-Mac-treated leukemia-bearing mice ($p < 0.001$) (Figure 6D-E). Consistent with the
333 MSC treatment, we also observed increased ratios of mature megakaryocytes ($p < 0.001$) (Figure
334 6F-G) and alleviated tumor burden ($CD11b^+$) (Figure S17) in E-Mac-treated leukemia-bearing
335 mice. Collectively, these results demonstrate that MSC-reprogrammed macrophages largely
336 recapitulate the therapeutic effects of MSCs.

337 **MSCs reprogram macrophages and reduce leukemia burden through IL-6**

338 Residual MSCs in leukemia-bearing mice lost the ability to secrete IL-6 (Figure 1G-H). IL-6 is
339 critical for maintaining the stemness and function of MSCs[60]. The recovered host MSCs after
340 donor MSC-treatment expressed comparable *Il6* mRNA as healthy MSCs (Figure 4E-G).
341 Consistently, BM plasma IL-6 levels in MSC-treated leukemia-bearing mice were significantly
342 elevated (> 3 folds) and were comparable to those in healthy mice ($p < 0.001$) (Figure 7A). To
343 investigate the biological consequence of reduced IL-6 on MSCs, we analyzed the MSCs in *Il6*$^{-/-}$
344 mice by *in vitro* proliferation assay. We observed that the *Il6*$^{-/-}$ MSCs proliferated at a significantly
345 slower speed than their WT counterparts *in vitro* ($p < 0.001$) (Figure. S18A). To investigate the
346 role of IL-6 in MSC-mediated therapeutic effects, we directly injected IL-6 proteins (40 μg/kg)
347 into leukemia-bearing mice. However, systemic IL-6 transfusion failed to suppress leukemia
348 (Figure S18B), which indicates that MSC-educated leukemic macrophages are distinct from the
349 conventional IL-6-dependent myeloid-derived immune-suppressor cells[61]. We speculated that IL-
350 6 might function as an autocrine factor for MSCs to reprogram macrophages in leukemia-bearing
351 mice. *In vitro* co-culture assay showed that *Il6*$^{-/-}$ MSCs compromised their ability to induce *Arg1*

352 expression in macrophages derived from leukemia-bearing mice (Figure 7B). In addition, intra-
353 BM injection of *Il6*$^{-/-}$ MSCs neither improved thrombopoiesis nor reduced tumor burden in
354 leukemia-bearing mice (Figure 7C-E). Furthermore, loss of *Il6* significantly compromised MSCs'
355 ability to reprogram leukemic macrophages, demonstrated by mild increase of the ratios of Arg1^{high}
356 macrophage subpopulation in *Il6*$^{-/-}$ MSC-treated leukemic mice *in vivo* (Figure 7F-H). Taken
357 together, these results demonstrate that autocrine IL-6 is essential for MSC-mediated
358 reprogramming of macrophages and reduction of tumor burden in leukemia-bearing mice.

359 **Discussion**

360 Deteriorating BM microenvironment accompanies chronic leukemia progression. Here we unravel
361 a *de novo* approach of reverting the impaired BM microenvironment by intra-BM injection of
362 donor MSCs. Upon injection, the donor MSCs quickly reprogrammed local host BM macrophages
363 to repair the niche, thus improving normal hematopoiesis and suppressing leukemia development.
364 These effects of donor MSCs depend on the autocrine production of IL-6. Our studies reveal de
365 novo mechanisms underlying MSC-mediated local BM microenvironment restoration that
366 systemically suppress leukemia development.

367 Given the short-term lifespan of the exogenous MSC *in vivo*, it is surprising that local injection of
368 donor MSCs results in long-term improvement of thrombopoiesis and reduction of tumor burden.
369 Following injection, exogenous donor MSCs immediately reprogram host resident macrophages
370 that further organize the overhaul of local BM microenvironment, including restoring the functions
371 of host MSCs. There is a lot of evidence supporting the pivotal roles of macrophages in tissue
372 repair[62,63]. Donor MSCs can transiently release a key wave of tissue-repair factors, such as IL-6[45],
373 CCL7[50], and CXCL12[47], and reprogram host macrophages, subsequently resulting in the recovery
374 of host MSCs. Recovered host MSCs further secreted much higher level of CCL2, CCL7, and

375 CXCL12 that can further facilitate BM niche repair. Donor MSCs could also directly modulate the
376 other niche cells, in addition to macrophages, to participate in BM niche repair[12]. Consequently,
377 the restored local BM microenvironment outputs abundant hematopoiesis-improving cytokines,
378 including IL-6[56], and reduces tumor-growth-stimulating cytokines, such as GM-CSF[27,55]. Thus,
379 despite the short life-span, donor MSCs provide long-term thrombopoiesis improvement and
380 tumor burden reduction through the stepwise microenvironment restoration.
381 Of note, IL-6 deficiency in MSCs markedly compromised the abilities of these cells to reprogram
382 host resident macrophage. Transwell co-culture study has shown that direct interaction between
383 MSCs and macrophages is a necessity for reprogramming host macrophages. Both autocrine
384 production of IL-6 and reprogramming host macrophages by MSCs are required for MSC-
385 mediated microenvironment restoration and leukemia inhibition. However, it is not clear how
386 autocrine IL-6 controls the function of MSCs and how MSCs directly reprogram macrophages.
387 The underlying molecular mechanisms warrant further investigation. Besides IL-6, it deserves
388 additional investigations of whether other key molecules produced by MSCs are involved in the
389 MSC-mediated microenvironment restoration and leukemia inhibition, such as nitric oxide[64].
390 MSC treatment inhibits leukemia development in the *Nras* mutation-induced MPN/MDS-like
391 disease model. We also attempted to broaden MSC treatment for acute leukemia in the MLL-AF9-
392 initiated model (Figure S19A), in which impaired MSCs results in the reduction of osteogenesis
393 and CXCL12 production[65]. Despite a mild elevation of platelet level, the intra-BM transfusion of
394 donor MSCs failed to significantly improve normal hematopoiesis or suppress acute leukemia
395 development (Figure S19B-H). Therefore, the intra-BM MSC treatment might be beneficial for
396 MPN/MDS leukemias, such as JMML and CMML, but insufficient for suppressing acute
397 leukemia. Although MSC application could be an effective therapeutic regimen for patients with

398 MPN/MDS-subtype leukemia, combination therapy of conventional approaches with local MSC
399 transfusion might be required to achieve therapeutic outcomes for acute leukemia with impaired
400 BM microenvironment.

401 **Acknowledgments**

402 This work was supported by grants from the Strategic Priority Research Program of Chinese
403 Academy of Sciences (XDA16010601), the Chinese Ministry of Science and Technology
404 (2015CB964401, 2016YFA0100601, 2016YFA0100600, 2017YFA0103401, and
405 2015CB964902), the Major Research and Development Project of Guangzhou Regenerative
406 Medicine and Health Guangdong Laboratory (2018GZR110104006, 2018GZR0201008), the CAS
407 Key Research Program of Frontier Sciences (QYZDB-SSW-SMC057), the Health and Medical
408 Care Collaborative Innovation Program of Guangzhou Scientific and Technology
409 (201803040017), CAMS Innovation Fund for Medical Sciences (2016-12M-1-002), the General
410 Program from Guangzhou Scientific and Technological Project (201707010157), the Science and
411 Technology Planning Project of Guangdong Province (2017B030314056, 2017B020230004), the
412 grants from the National Natural Science Foundation of China (Grant No 31471117, 31271457,
413 81470281, 81421002, 81730006, 31600948, and 81861148029), the CAMS Initiative for
414 Innovative Medicine (2016-I2M-1-017) and the grants from NIH, USA (AI079087, D.W. and
415 HL130724 D.W.)

416 **Author Contributions**

417 C.X.X. performed research, analyzed data and wrote the manuscript; D.Y. and Q.T.W. analyzed
418 RNA-Seq data; T.J.W., H.C., P.Q.Z., K.T.W., X.F.L., Y.G., S.H.M., L.X. and Y.X.G. performed
419 experiments; S.H., J.D., X.D., Y.Q.L., X.F.Z., Y.F.S. and S.X. discussed the manuscript; D.W.

420 discussed the project and wrote the manuscript. T.C. and J.Y.W. designed the research and wrote
421 the manuscript.

422 **Conflict of Interest Disclosure**

423 The authors declare no competing financial interests.

424 **References**

425 1. Kfoury Y, Scadden DT. Mesenchymal cell contributions to the stem cell niche. *Cell Stem Cell*.
426 2015;16(3):239-253.

427 2. Lim M, Pang Y, Ma S, et al. Altered mesenchymal niche cells impede generation of normal
428 hematopoietic progenitor cells in leukemic bone marrow. *Leukemia*. 2016;30(1):154-162.

429 3. Raaijmakers MH, Mukherjee S, Guo S, et al. Bone progenitor dysfunction induces myelodysplasia
430 and secondary leukaemia. *Nature*. 2010;464(7290):852-857.

431 4. Schepers K, Pietras EM, Reynaud D, et al. Myeloproliferative neoplasia remodels the endosteal
432 bone marrow niche into a self-reinforcing leukemic niche. *Cell Stem Cell*. 2013;13(3):285-299.

433 5. Bowers M, Zhang B, Ho Y, Agarwal P, Chen CC, Bhatia R. Osteoblast ablation reduces normal
434 long-term hematopoietic stem cell self-renewal but accelerates leukemia development. *Blood*.
435 2015;125(17):2678-2688.

436 6. Dong L, Yu WM, Zheng H, et al. Leukaemogenic effects of Ptpn11 activating mutations in the
437 stem cell microenvironment. *Nature*. 2016;539(7628):304-308.

438 7. Blau O, Baldus CD, Hofmann WK, et al. Mesenchymal stromal cells of myelodysplastic syndrome
439 and acute myeloid leukemia patients have distinct genetic abnormalities compared with leukemic blasts.
440 *Blood*. 2011;118(20):5583-5592.

441 8. Pandis N, Bardi G, Sfikas K, Panayotopoulos N, Tserkezoglou A, Fotiou S. Complex chromosome
442 rearrangements involving 12q14 in two uterine leiomyomas. *Cancer Genet Cytogenet*. 1990;49(1):51-56.

443 9. Medyouf H, Mossner M, Jann JC, et al. Myelodysplastic cells in patients reprogram mesenchymal
444 stromal cells to establish a transplantable stem cell niche disease unit. *Cell Stem Cell*. 2014;14(6):824-837.
445 10. Ren G, Zhang L, Zhao X, et al. Mesenchymal stem cell-mediated immunosuppression occurs via
446 concerted action of chemokines and nitric oxide. *Cell Stem Cell*. 2008;2(2):141-150.
447 11. Prockop DJ. Inflammation, fibrosis, and modulation of the process by mesenchymal stem/stromal
448 cells. *Matrix Biol*. 2016;51:7-13.
449 12. Shi Y, Wang Y, Li Q, et al. Immunoregulatory mechanisms of mesenchymal stem and stromal cells
450 in inflammatory diseases. *Nat Rev Nephrol*. 2018;14(8):493-507.
451 13. Le Blanc K, Mougiakakos D. Multipotent mesenchymal stromal cells and the innate immune
452 system. *Nat Rev Immunol*. 2012;12(5):383-396.
453 14. Mittal M, Tiruppathi C, Nepal S, et al. TNFalpha-stimulated gene-6 (TSG6) activates macrophage
454 phenotype transition to prevent inflammatory lung injury. *Proc Natl Acad Sci U S A*. 2016;113(50):E8151-
455 E8158.
456 15. Wang G, Cao K, Liu K, et al. Kynurenic acid, an IDO metabolite, controls TSG-6-mediated
457 immunosuppression of human mesenchymal stem cells. *Cell Death Differ*. 2018;25(7):1209-1223.
458 16. Du L, Lin L, Li Q, et al. IGF-2 Preprograms Maturing Macrophages to Acquire Oxidative
459 Phosphorylation-Dependent Anti-inflammatory Properties. *Cell Metab*. 2019.
460 17. Eggenhofer E, Benseler V, Kroemer A, et al. Mesenchymal stem cells are short-lived and do not
461 migrate beyond the lungs after intravenous infusion. *Front Immunol*. 2012;3:297.
462 18. Ehninger A, Trumpp A. The bone marrow stem cell niche grows up: mesenchymal stem cells and
463 macrophages move in. *J Exp Med*. 2011;208(3):421-428.
464 19. Chen J, Yao Y, Gong C, et al. CCL18 from tumor-associated macrophages promotes breast cancer
465 metastasis via PITPNM3. *Cancer Cell*. 2011;19(4):541-555.
466 20. Gubin MM, Esaulova E, Ward JP, et al. High-Dimensional Analysis Delineates Myeloid and
467 Lymphoid Compartment Remodeling during Successful Immune-Checkpoint Cancer Therapy. *Cell*.
468 2018;175(4):1014-1030 e1019.

469 21. Chen CC, Wang L, Plikus MV, et al. Organ-level quorum sensing directs regeneration in hair stem
470 cell populations. *Cell*. 2015;161(2):277-290.
471 22. Liu C, Wu C, Yang Q, et al. Macrophages Mediate the Repair of Brain Vascular Rupture through
472 Direct Physical Adhesion and Mechanical Traction. *Immunity*. 2016;44(5):1162-1176.
473 23. Winkler IG, Sims NA, Pettit AR, et al. Bone marrow macrophages maintain hematopoietic stem
474 cell (HSC) niches and their depletion mobilizes HSCs. *Blood*. 2010;116(23):4815-4828.
475 24. Bosurgi L, Cao YG, Cabeza-Cabrerizo M, et al. Macrophage function in tissue repair and
476 remodeling requires IL-4 or IL-13 with apoptotic cells. *Science*. 2017;356(6342):1072-1076.
477 25. Cho DI, Kim MR, Jeong HY, et al. Mesenchymal stem cells reciprocally regulate the M1/M2
478 balance in mouse bone marrow-derived macrophages. *Exp Mol Med*. 2014;46:e70.
479 26. Nemeth K, Leelahavanichkul A, Yuen PS, et al. Bone marrow stromal cells attenuate sepsis via
480 prostaglandin E(2)-dependent reprogramming of host macrophages to increase their interleukin-10
481 production. *Nat Med*. 2009;15(1):42-49.
482 27. Wang J, Liu Y, Li Z, et al. Endogenous oncogenic Nras mutation promotes aberrant GM-CSF
483 signaling in granulocytic/monocytic precursors in a murine model of chronic myelomonocytic leukemia.
484 *Blood*. 2010;116(26):5991-6002.
485 28. Wang J, Liu Y, Li Z, et al. Endogenous oncogenic Nras mutation initiates hematopoietic
486 malignancies in a dose- and cell type-dependent manner. *Blood*. 2011;118(2):368-379.
487 29. Wang JY, Kong GY, Liu YG, et al. Nras(G12D/+) promotes leukemogenesis by aberrantly
488 regulating hematopoietic stem cell functions. *Blood*. 2013;121(26):5203-5207.
489 30. Tang F, Barbacioru C, Nordman E, et al. RNA-Seq analysis to capture the transcriptome landscape
490 of a single cell. *Nat Protoc*. 2010;5(3):516-535.
491 31. Kim D, Langmead B, Salzberg SL. HISAT: a fast spliced aligner with low memory requirements.
492 *Nat Methods*. 2015;12(4):357-360.
493 32. Liao Y, Smyth GK, Shi W. featureCounts: an efficient general purpose program for assigning
494 sequence reads to genomic features. *Bioinformatics*. 2014;30(7):923-930.

495 33. Love MI, Huber W, Anders S. Moderated estimation of fold change and dispersion for RNA-seq
496 data with DESeq2. *Genome Biol*. 2014;15(12):550.
497 34. Subramanian A, Tamayo P, Mootha VK, et al. Gene set enrichment analysis: a knowledge-based
498 approach for interpreting genome-wide expression profiles. *Proc Natl Acad Sci U S A*. 2005;102(43):15545-
499 15550.
500 35. Yu G, Wang LG, Han Y, He QY. clusterProfiler: an R package for comparing biological themes
501 among gene clusters. *OMICS*. 2012;16(5):284-287.
502 36. Freeman BT, Jung JP, Ogle BM. Single-Cell RNA-Seq of Bone Marrow-Derived Mesenchymal
503 Stem Cells Reveals Unique Profiles of Lineage Priming. *PLoS One*. 2015;10(9):e0136199.
504 37. Song L, Webb NE, Song Y, Tuan RS. Identification and functional analysis of candidate genes
505 regulating mesenchymal stem cell self-renewal and multipotency. *Stem Cells*. 2006;24(7):1707-1718.
506 38. Rostovskaya M, Anastassiadis K. Differential expression of surface markers in mouse bone marrow
507 mesenchymal stromal cell subpopulations with distinct lineage commitment. *PLoS One*.
508 2012;7(12):e51221.
509 39. Delorme B, Ringe J, Pontikoglou C, et al. Specific lineage-priming of bone marrow mesenchymal
510 stem cells provides the molecular framework for their plasticity. *Stem Cells*. 2009;27(5):1142-1151.
511 40. Medina RJ, O'Neill CL, O'Doherty TM, et al. Myeloid angiogenic cells act as alternative M2
512 macrophages and modulate angiogenesis through interleukin-8. *Mol Med*. 2011;17(9-10):1045-1055.
513 41. Arango Duque G, Descoteaux A. Macrophage cytokines: involvement in immunity and infectious
514 diseases. *Front Immunol*. 2014;5:491.
515 42. Cavaillon JM. Cytokines and macrophages. *Biomed Pharmacother*. 1994;48(10):445-453.
516 43. Li Q, Haigis KM, McDaniel A, et al. Hematopoiesis and leukemogenesis in mice expressing
517 oncogenic NrasG12D from the endogenous locus. *Blood*. 2011;117(6):2022-2032.
518 44. Gnecchi M, Danieli P, Malpasso G, Ciuffreda MC. Paracrine Mechanisms of Mesenchymal Stem
519 Cells in Tissue Repair. *Methods Mol Biol*. 2016;1416:123-146.

520 45. Gallucci RM, Simeonova PP, Matheson JM, et al. Impaired cutaneous wound healing in
521 interleukin-6-deficient and immunosuppressed mice. *FASEB J*. 2000;14(15):2525-2531.
522 46. Castela M, Nassar D, Sbeih M, Jachiet M, Wang Z, Aractingi S. Ccl2/Ccr2 signalling recruits a
523 distinct fetal microchimeric population that rescues delayed maternal wound healing. *Nat Commun*.
524 2017;8:15463.
525 47. Kato T, Khanh VC, Sato K, et al. SDF-1 improves wound healing ability of glucocorticoid-treated
526 adipose tissue-derived mesenchymal stem cells. *Biochem Biophys Res Commun*. 2017;493(2):1010-1017.
527 48. Hayashi Y, Murakami M, Kawamura R, Ishizaka R, Fukuta O, Nakashima M. CXCL14 and MCP1
528 are potent trophic factors associated with cell migration and angiogenesis leading to higher regenerative
529 potential of dental pulp side population cells. *Stem Cell Res Ther*. 2015;6:111.
530 49. Sims NA, Jenkins BJ, Nakamura A, et al. Interleukin-11 receptor signaling is required for normal
531 bone remodeling. *J Bone Miner Res*. 2005;20(7):1093-1102.
532 50. Schenk S, Mal N, Finan A, et al. Monocyte chemotactic protein-3 is a myocardial mesenchymal
533 stem cell homing factor. *Stem Cells*. 2007;25(1):245-251.
534 51. Kleppe M, Kwak M, Koppikar P, et al. JAK-STAT pathway activation in malignant and
535 nonmalignant cells contributes to MPN pathogenesis and therapeutic response. *Cancer Discov*.
536 2015;5(3):316-331.
537 52. Pang L, Weiss MJ, Poncz M. Megakaryocyte biology and related disorders. *J Clin Invest*.
538 2005;115(12):3332-3338.
539 53. Zhu H, Guo ZK, Jiang XX, et al. A protocol for isolation and culture of mesenchymal stem cells
540 from mouse compact bone. *Nat Protoc*. 2010;5(3):550-560.
541 54. Rombouts WJ, Ploemacher RE. Primary murine MSC show highly efficient homing to the bone
542 marrow but lose homing ability following culture. *Leukemia*. 2003;17(1):160-170.
543 55. Padron E, Painter JS, Kunigal S, et al. GM-CSF-dependent pSTAT5 sensitivity is a feature with
544 therapeutic potential in chronic myelomonocytic leukemia. *Blood*. 2013;121(25):5068-5077.

545 56. Kaser A, Brandacher G, Steurer W, et al. Interleukin-6 stimulates thrombopoiesis through
546 thrombopoietin: role in inflammatory thrombocytosis. *Blood*. 2001;98(9):2720-2725.
547 57. de Lima M, McNiece I, Robinson SN, et al. Cord-blood engraftment with ex vivo mesenchymal-
548 cell coculture. *N Engl J Med*. 2012;367(24):2305-2315.
549 58. Ohnishi H, Kobayashi H, Okazawa H, et al. Ectodomain shedding of SHPS-1 and its role in
550 regulation of cell migration. *J Biol Chem*. 2004;279(27):27878-27887.
551 59. Hocking AM. The Role of Chemokines in Mesenchymal Stem Cell Homing to Wounds. *Adv*
552 *Wound Care (New Rochelle)*. 2015;4(11):623-630.
553 60. Pricola KL, Kuhn NZ, Haleem-Smith H, Song Y, Tuan RS. Interleukin-6 maintains bone marrow-
554 derived mesenchymal stem cell stemness by an ERK1/2-dependent mechanism. *J Cell Biochem*.
555 2009;108(3):577-588.
556 61. Marigo I, Bosio E, Solito S, et al. Tumor-induced tolerance and immune suppression depend on
557 the C/EBPbeta transcription factor. *Immunity*. 2010;32(6):790-802.
558 62. Wynn TA, Vannella KM. Macrophages in Tissue Repair, Regeneration, and Fibrosis. *Immunity*.
559 2016;44(3):450-462.
560 63. Liu C, Wu CA, Yang QF, et al. Macrophages Mediate the Repair of Brain Vascular Rupture through
561 Direct Physical Adhesion and Mechanical Traction. *Immunity*. 2016;44(5):1162-1176.
562 64. Trento C, Marigo I, Pievani A, et al. Bone marrow mesenchymal stromal cells induce nitric oxide
563 synthase-dependent differentiation of CD11b(+) cells that expedite hematopoietic recovery.
564 *Haematologica*. 2017;102(5):818-825.
565 65. Hanoun M, Zhang D, Mizoguchi T, et al. Acute myelogenous leukemia-induced sympathetic
566 neuropathy promotes malignancy in an altered hematopoietic stem cell niche. *Cell Stem Cell*.
567 2014;15(3):365-375.
568

569 **Figures and figure legends**

Figure 1

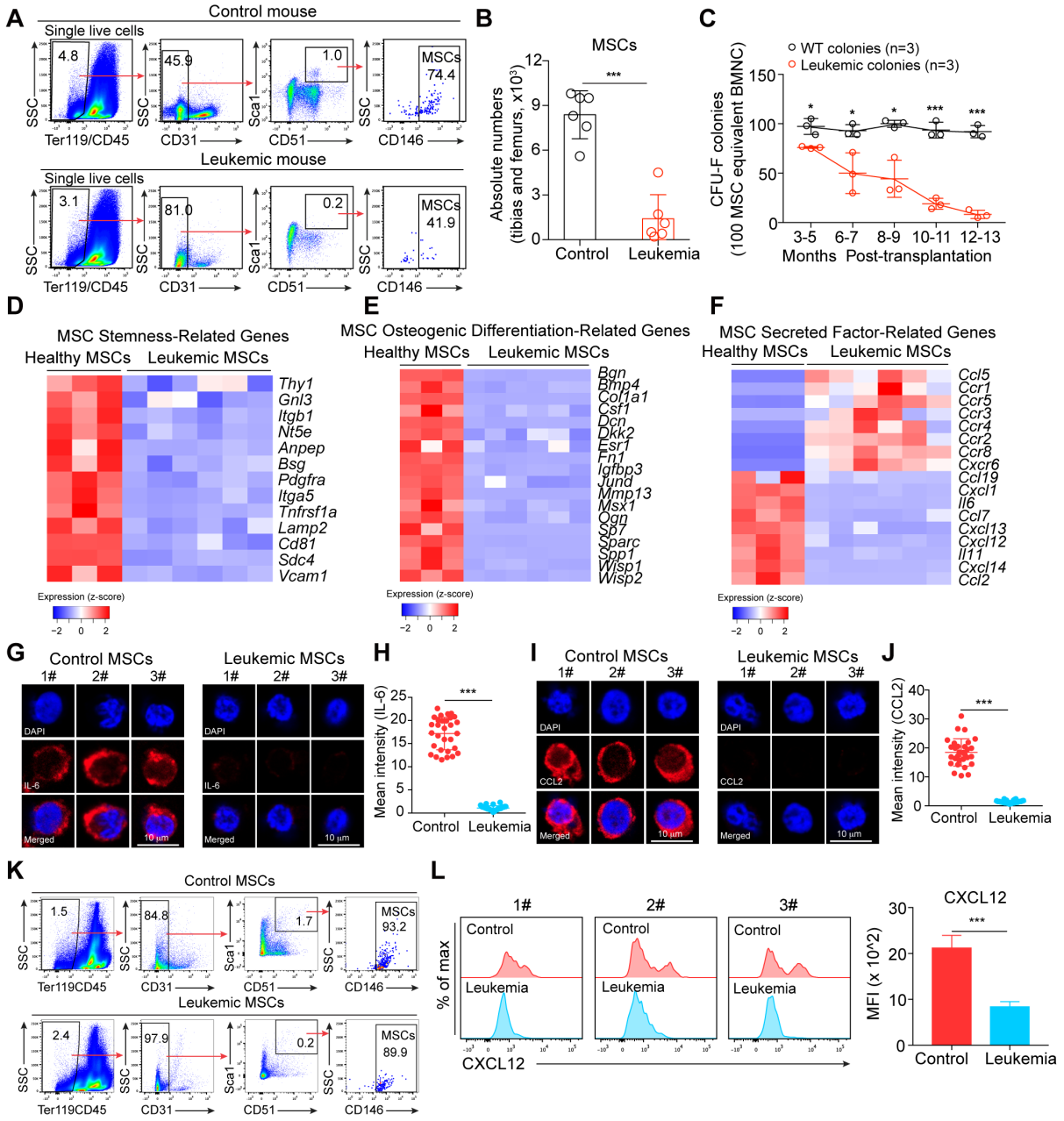

570

571 **Figure 1: Impaired BM MSCs in mice with NrasG12D mutation-induced leukemia**

572 CD45.2$^+$ BMNC from LSL *Nras*/+; *Vav-Cre* mice (NV mice) were sorted and transplanted into

573 sublethally irradiated (6.5 Gy) individual recipients (CD45.1 strain) with a cell dose of 0.3 million

574 per recipient. For control recipient mice (CD45.1 strain), 0.3 million sorted CD45.2$^+$ BMNC from

575 WT mice were transplanted. **(A)** Gating strategies for BM MSCs. MSCs are defined as Ter119$^-$
576 CD45$^-$CD31$^-$Sca1$^+$CD51$^+$ CD146$^+$. Plots from one representative control mouse (CD11b$^+$% in PB
577 = 10%) and one leukemia-bearing mouse (CD11b$^+$% in PB > 60%) of six mice of each group are
578 shown. The nucleated cell mixtures of BM and compact bones were prepared for flow cytometry
579 analysis of MSCs. **(B)** Statistical analysis of the absolute numbers of MSCs in tibias and femurs
580 from control and leukemia-bearing mice. Data are analyzed by unpaired student's t-test (two-
581 tailed). ***p < 0.001. Data are represented as mean ± SD (n = 6 mice for each group from multiple
582 independent experiments). **(C)** Kinetic analysis of functional MSCs in CFU-F assay. Total BMNC
583 equivalent to 100 MSCs calculated by the percentages of MSCs in individual BMNC samples by
584 flow cytometry analysis. Data are analyzed by unpaired student's t-test (two-tailed). *p < 0.05,
585 ***p < 0.001. For each time point, three independent experiments were performed. Data are
586 represented as mean ± SD. **(D)** Heatmaps of MSC stemness-related genes differentially expressed
587 between healthy MSCs and MSCs from leukemia-bearing mice (padj < 0.05, fold change > 1.6).
588 One thousand sorted MSCs (Ter119$^-$CD45$^-$CD31$^-$Sca1$^+$CD51$^+$) from the nucleated cell mixtures
589 of BM and compact bones of independent leukemia-bearing mice, control mice, and MSC-treated
590 leukemia-bearing mice were used as each cell sample input for RNA-Seq. Leukemia-bearing mice
591 (CD11b$^+$% in PB = 35%-45%) and control mice (CD11b$^+$% in PB = 10-15%) were accumulated
592 from multiple independent experiments. The expression value (DESeq2 normalized counts) of
593 each gene was converted to z-score values (red, high; blue, low), and the heatmaps were plotted
594 by gplots (heatmap.2). Columns represent the indicated cell subsets in nine MSC samples (Healthy
595 MSCs from control mice: n = 3, MSCs from leukemia-bearing mice: n = 6). **(E)** Heatmaps of
596 osteogenic differentiation-related genes differentially expressed between healthy MSCs and MSCs
597 from leukemia-bearing mice (padj < 0.05, fold change > 2). The expression value (DESeq2

598 normalized counts) of each gene was converted to z-score values (red, high; blue, low), and the
599 heatmaps were plotted by gplots (heatmap.2). Columns represent the indicated cell subsets in nine
600 MSC samples (Healthy MSCs: n = 3, MSCs from leukemia-bearing mice: n = 6). **(F)** Heatmaps of
601 MSC secreted factor-related genes differentially expressed between healthy MSCs and MSCs from
602 leukemia-bearing mice (padj < 0.05, fold change > 2). The expression value (DESeq2 normalized
603 counts) of each gene was converted to z-score values (red, high; blue, low), and the heatmaps were
604 plotted by gplots (heatmap.2). Columns represent the indicated cell subsets in nine MSC samples
605 (Healthy MSCs: n = 3, MSCs from leukemia-bearing mice: n = 6). **(G)** Single-cell imaging of
606 intracellular IL-6 proteins by indirect immunofluorescence assay (IFA) in primary MSCs sorted
607 from the control and leukemic mice. Images of three single representative cells of each group are
608 shown. **(H)** Statistical analysis of mean intensities of IL-6 fluorescence in control and leukemic
609 MSC samples. Each dot represents a single cell. Data are analyzed by unpaired student's t-test
610 (two-tailed). ***p < 0.001. Data are represented as mean ± SD. Control, n=30; Leukemia, n=30.
611 **(I)** Single-cell imaging of intracellular CCL2 proteins by IFA in primary MSCs sorted from the
612 control and leukemic mice. Images of three single representative cells of each group are shown.
613 **(J)** Statistical analysis of mean intensities of CCL2 fluorescence in control and leukemic MSC
614 samples. Each dot represents a single cell. Data are analyzed by unpaired student's t-test (two-
615 tailed). ***p < 0.001. Data are represented as mean ± SD. Control, n=30; Leukemia, n=30. **(K)**
616 Representative intracellular staining plots of CXCL12 proteins in control and leukemic MSCs
617 analyzed by flow cytometry. **(L)** Statistical analysis of mean fluorescence intensities (MFI) of
618 CXCL12 in control and leukemic MSCs. Data are analyzed by unpaired student's t-test (two-
619 tailed). ***p < 0.001. Plots from three representative control mice and leukemia-bearing mice are
620 shown. Data are represented as mean ± SD (n = 6 mice for each group).

Figure 2

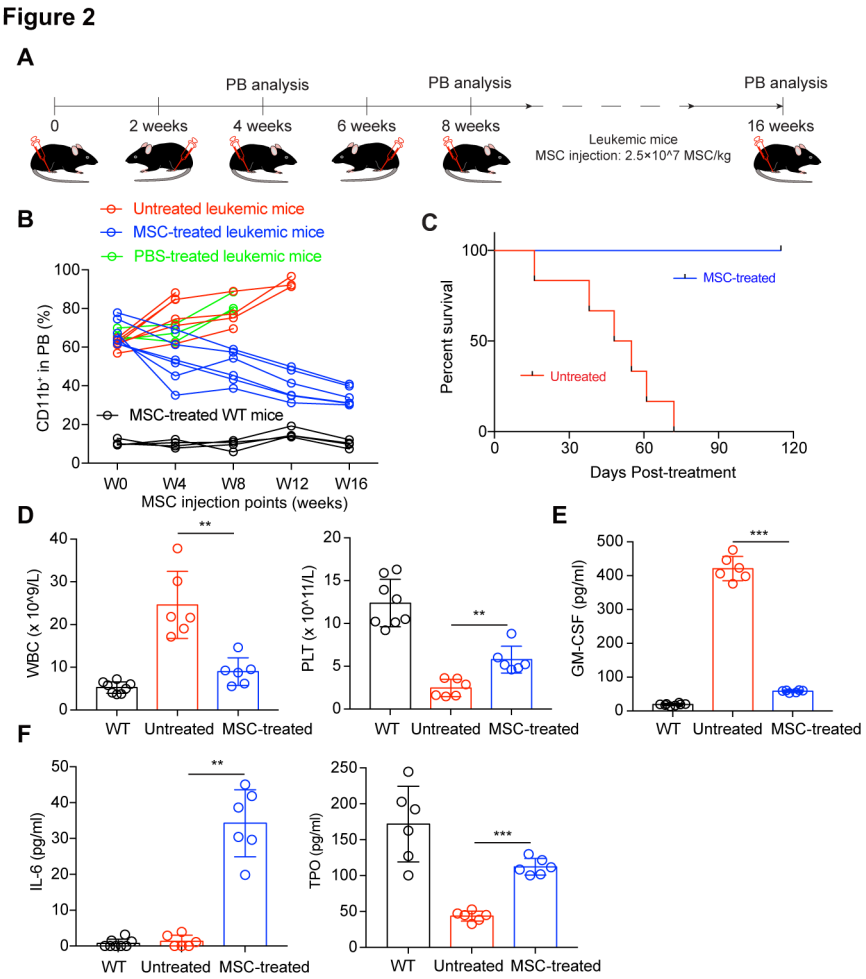

Figure 2: Intra-BM transfusion of donor MSCs prolongs survival of leukemia-bearing mice **(A)** Schematic diagram of MSC transfusion strategy. The donor MSCs prepared for transfusion were isolated from the compact bone and BMNC of three to four-week-old healthy GFP mice. The isolated MSCs were expanded *in vitro*, and the secondary passage products were used for transfusion. Leukemia-bearing mice with severe tumor burden (CD11b$^+$% in PB > 60%) were treated by intra-bone-marrow transfusion of donor MSCs. WT mice were treated by the same procedure as treatment control, and leukemia-bearing mice without MSC treatment were used as untreated controls. A sequential doses of MSCs (2.5 × 10^7 MSCs/kg per dose in 20 μL DPBS) were delivered into the tibia cavity using 29-gauge needle. Every tibia was treated once per month by switching the injection site every other dose. **(B)** Kinetic analysis of tumor burden (CD11b$^+$) of

632 MSC-treated leukemia-bearing mice. The time window of MSC treatment is from 0 weeks (W0,
633 treatment starting time) to 16 weeks (W16). Flow cytometry analysis of tumor burden ($CD11b^+$)
634 in PB was performed monthly. These leukemia-bearing mice were accumulated from multiple
635 independent experiments. The individual leukemia-bearing mice were selected to perform
636 treatment once they reached the leukemic burden standard ($CD11b^+$% > 60% in peripheral blood),
637 but at different time from multiple experiments. Untreated leukemia-bearing mice were used as
638 disease control (red line), PBS-treated leukemia-bearing mice were used as injected control (green
639 line), and MSC-treated WT mice were used as treatment control (black line). Untreated leukemia-
640 bearing mice: n = 6; PBS-treated leukemia-bearing mice: n = 3; MSC-treated leukemia-bearing
641 mice (blue line): n = 6; MSC-treated WT mice: n = 4. **(C)** Kaplan-Meier survival of MSC-treated
642 leukemia-bearing mice. Kaplan-Meier survival curves of untreated (n = 6, Median survival = 51.5
643 days) and MSC-treated (n = 6, Median survival = 115 days) leukemia-bearing mice are shown.
644 MSC treatment was terminated after 16 weeks. The untreated leukemia-bearing mice from the
645 same batch were used as control (red line). Log-rank (Mantel-Cox) test: $p < 0.001$. **(D)** Statistical
646 analysis of white blood cells (WBC) and platelets (PLT) counts in PB of WT mice, untreated
647 leukemia-bearing mice, and MSC-treated leukemia-bearing mice at week nine since the MSC
648 treatment. Data are analyzed by one-way ANOVA test. $^{**}p < 0.01$. Data are represented as mean
649 ± SD (n =6-8 mice for each group). **(E)** ELISA of GM-CSF levels in PB serum. Serum prepared
650 from 200 μL PB of individual WT mice (n=8), untreated leukemia-bearing mice (Untreated, n=6)
651 and MSC-treated leukemia-bearing mice (MSC-treated, n=6) eight weeks post MSC treatment.
652 Data are analyzed by one-way ANOVA test. $^{***}p < 0.001$. Data are represented as mean ± SD.
653 **(F)** ELISA of IL-6 and TPO levels in PB serum. Serum prepared from 200 μL PB of individual
654 WT mice (n=6-8), untreated leukemia-bearing mice (Untreated, n=6) and MSC-treated leukemia-

655 bearing mice (MSC-treated, n=6) eight weeks post MSC treatment. Data are analyzed by one-way

656 ANOVA. **$p < 0.01$, ***$p < 0.001$. Data are represented as mean ± SD.

657

Figure 3

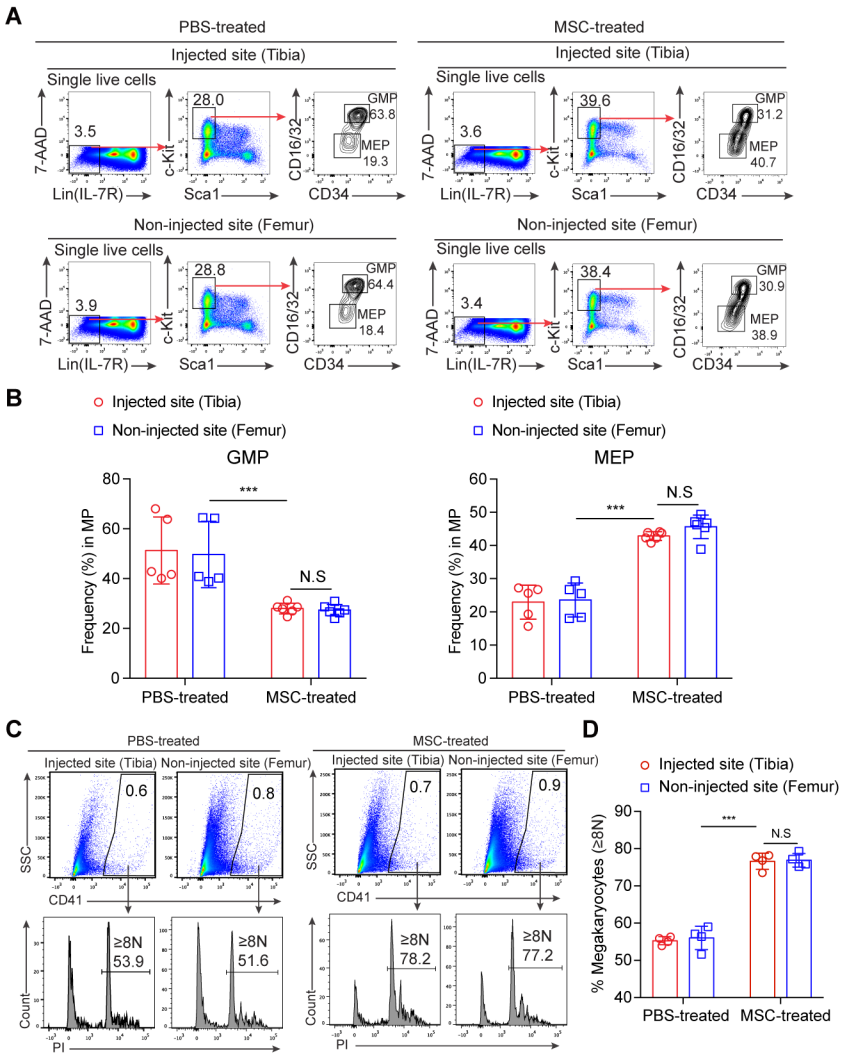

658

659 **Figure 3: Systemically re-balanced myeloid lineage progenitor cells and systemically**

660 **activated megakaryocytes in MSC-treated leukemia-bearing mice**

661 **(A)** Ratios of myeloid progenitor subpopulations in MSC- and PBS-treated leukemia-bearing

662 mice. Total bone marrow nucleated cells were from the MSC-injected site (tibia) and non-injected

663 site (femur) of each leukemia-bearing mouse, or PBS-injected site (tibia) and non-injected site

664 (femur) of each leukemia-bearing mouse four weeks post MSC/PBS treatment. GMP

665 (granulocyte/macrophage progenitors): $Lin^{-}IL\text{-}7R^{-}Sca1^{-}c\text{-}Kit^{+}CD34^{+}CD16/32^{high}$; MEP

666 (megakaryocyte/erythroid progenitors): $Lin^{-}IL\text{-}7R^{-}Sca1^{-}c\text{-}Kit^{+}CD34^{-}CD16/32^{-}$. **(B)** Statistical

667 analysis of myeloid progenitor components (GMP and MEP) in the injected site (tibia) and non-
668 injected site (femur) of each PBS-treated leukemia-bearing mouse and MSC-treated leukemia-
669 bearing mouse four weeks post-MSC treatment. Data are analyzed by one-way ANOVA test. ***p
670 < 0.001. Data are represented as mean ± SD (n = 5-6 mice for each group accumulated from
671 multiple independent experiments). **(C)** Activation analysis of megakaryocytes in MSC- and PBS-
672 treated leukemia-bearing mice. Plots from one representative PBS-treated leukemia-bearing
673 mouse and MSC-treated leukemia-bearing mouse four weeks post MSC treatment are shown.
674 Percentages of mature megakaryocytes with 8N and greater ploidy (≥8N) are shown. **(D)**
675 Statistical analysis of the percentages of mature megakaryocytes (≥8N). Data are analyzed by one-
676 way ANOVA test. ***p < 0.001, N.S indicates not-significant. Data are represented as mean ± SD
677 (n = 4 mice for each group accumulated from multiple independent experiments).
678

Figure 4

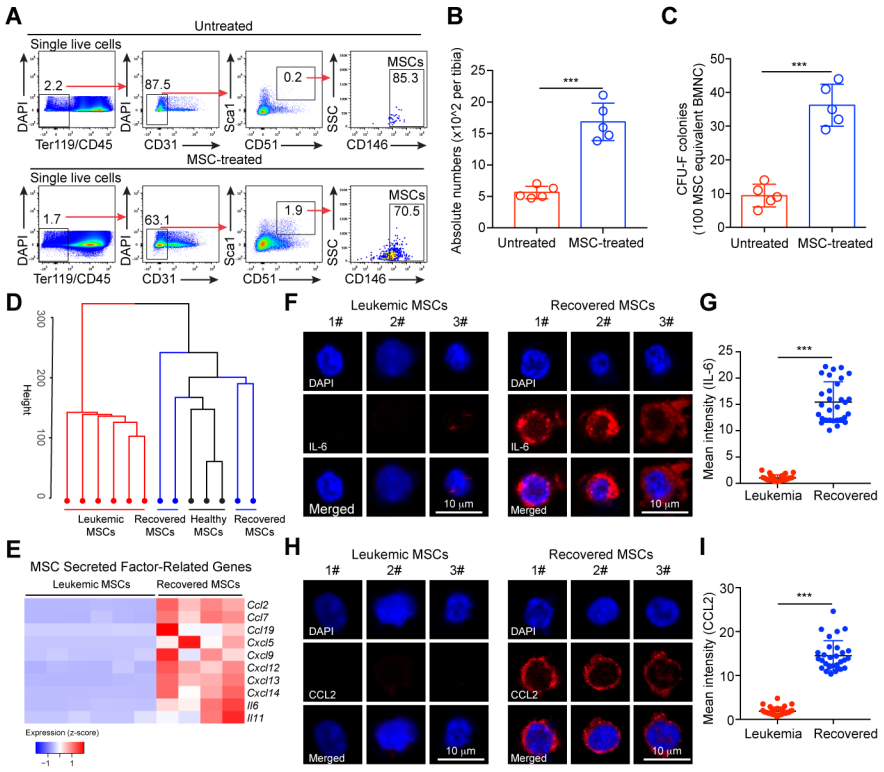

Figure 4: Characterization of recovered host MSCs from MSC-treated leukemia-bearing mice

(A) Flow cytometry analysis of recovered host MSCs in leukemia-bearing mice eight weeks post MSC treatment. Tibias of MSC-treated leukemia-bearing mice eight weeks after the first dose MSC treatment were analyzed. The leukemic mice are induced as described in Figure 1. The data of the MSC-treated tibias (injected sites) from MSC-treated leukemic mice and the control tibias from untreated leukemic mice are shown. Plots of one representative mouse from each group are shown. MSCs are defined as $Ter119^{-}CD45^{-}CD31^{-}Sca1^{+}CD51^{+}CD146^{+}$. The nucleated cell mixtures of BM and compact bones were prepared for flow cytometry analysis of MSCs. **(B)** Statistical analysis of the absolute numbers of host MSCs (GFP^{-}, host-derived MSCs) in tibias from untreated and MSC-treated leukemia-bearing mice. Data are analyzed by unpaired student's t-test (two-tailed). ***$p < 0.001$. Data are represented as mean ± SD (n = 5 mice for each group).

692 **(C)** Statistical analysis of CFU-F colonies. The numbers of colonies of each group were counted
693 after Giemsa staining. Data are analyzed by unpaired student's t-test (two-tailed). ***$p < 0.001$.
694 Data are represented as mean ± SD (n = 5 mice for each group). **(D)** Unsupervised hierarchical
695 clustering of RNA-Seq data of MSCs from leukemia-bearing mice, healthy MSCs, and recovered
696 MSCs (GFP^-, recipient-derived). For each RNA-Seq sample, one thousand MSCs from leukemia-
697 bearing mice, healthy mice, and MSC-treated leukemia-bearing mice were sorted and analyzed (n
698 = 3-6). The raw reads (fastq files) from RNA-Seq were aligned to mouse genome by Tophat2
699 package, and further normalized by Cufflinks. Unsupervised hierarchical clustering was conducted
700 by factoextra R package. **(E)** Heatmaps of MSC secreted factor-related genes differentially
701 expressed between MSCs from leukemia-bearing mice and recovered MSCs (padj < 0.05, fold
702 change > 1.4). The expression value (DESeq2 normalized counts) of each gene was converted to
703 z-score values (red, high; blue, low), and the heatmaps were plotted by gplots (heatmap.2).
704 Columns represent the indicated cell subsets in ten MSC samples (Leukemic MSCs: n = 6,
705 Recovered MSCs: n = 4). **(F)** Single-cell imaging of intracellular IL-6 proteins by indirect
706 immunofluorescence assay (IFA) in primary MSCs sorted from non-injected sites (Leukemic
707 MSCs) and MSC-injected sites (Recovered MSCs) of MSC-treated leukemic mice. Images of three
708 single representative cells of each group are shown. **(G)** Statistical analysis of mean intensities of
709 IL-6 fluorescence in leukemic and recovered MSC samples. Each dot represents a single cell. Data
710 are analyzed by unpaired student's t-test (two-tailed). ***$p < 0.001$. Data are represented as mean
711 ± SD. Control, n=30; Leukemia, n=30. **(H)** Single-cell imaging of intracellular CCL2 proteins by
712 IFA in primary MSCs sorted from non-injected sites (Leukemic MSCs) and MSC-injected sites
713 (Recovered MSCs) of MSC-treated leukemic mice. Images of three single representative cells of
714 each group are shown. **(I)** Statistical analysis of mean intensities of CCL2 fluorescence in leukemic

715 and recovered MSC samples. Each dot represents a single cell. Data are analyzed by unpaired
716 student's t-test (two-tailed). ***$p < 0.001$. Data are represented as mean ± SD. Control, n=30;
717 Leukemia, n=30.
718

Figure 5

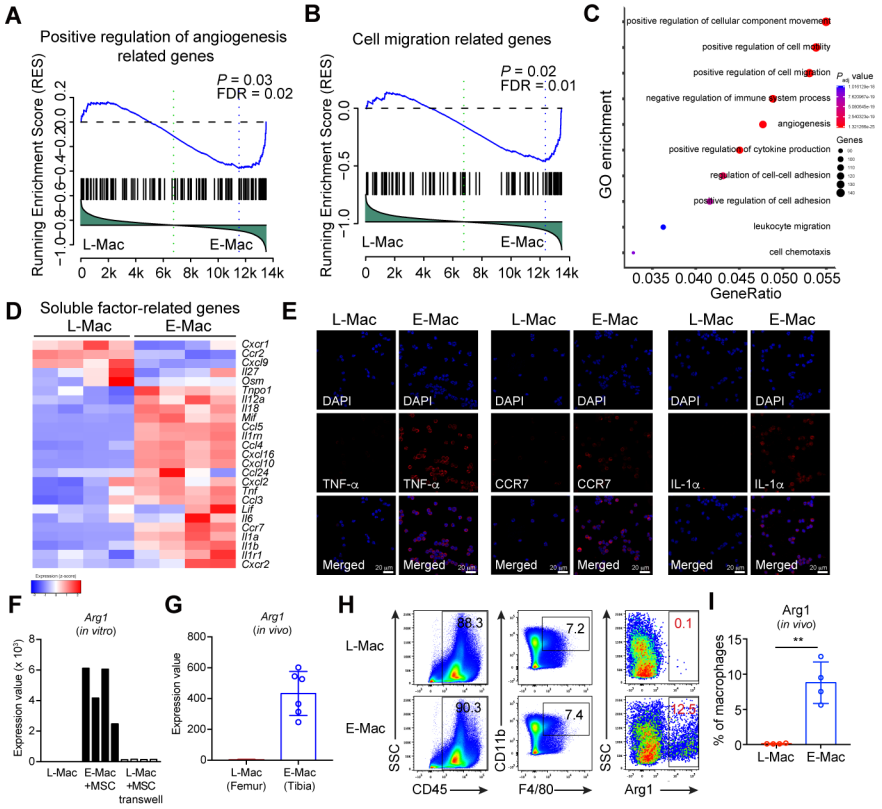

Figure 5: Characterization of MSC-reprogrammed BM resident macrophages isolated from leukemia-bearing mice

(A) Gene set enrichment analysis (GSEA) of the positive regulation of angiogenesis in L-Mac and E-Mac. L-Mac indicates leukemic macrophages. E-Mac indicates MSC-reprogrammed leukemic macrophages, which were co-cultured with MSCs *in vitro* for 12 h. DESeq2 normalized values of the expression data were used for GSEA analysis. **(B)** Gene set enrichment analysis (GSEA) of the cell migration-related genes in L-Mac and E-Mac. DESeq2 normalized values of the expression data were used for GSEA analysis. **(C)** Gene ontology (GO)–enrichment analysis of the 3277 differentially expressed genes between L-Mac and E-Mac: each symbol represents a GO term (noted in the plot); color indicates adjusted P value (padj (significance of the GO term)), and symbol size is proportional to the number of genes. **(D)** Heatmaps of soluble factor-related genes in MSC-reprogrammed leukemic macrophages. The expression value (DESeq2 normalized

732 counts) of each gene was converted to z-score value (red, high; blue, low). The heatmaps were
733 plotted by gplots (heatmap.2). Columns represent the indicated macrophage sample replicates (L-
734 Mac: n = 4 biological replicates; E-Mac: n = 4 biological replicates). **(E)** Imaging of intracellular
735 TNF-α, CCR7, and IL-1α proteins by indirect immunofluorescence assay (IFA) in sorted L-Mac
736 (Non-injected site) and E-Mac (MSC-injected site) from MSC-treated leukemic mice 12 h post-
737 treatment *in vivo*. The representative images of each group are shown. **(F)** RNA-Seq analysis of
738 *Arg1* in leukemic macrophages co-cultured with MSCs *in vitro.* L-Mac indicates leukemic
739 macrophages. E-Mac (+MSCs) indicates MSC-reprogrammed leukemic macrophages, which were
740 co-cultured with MSCs *in vitro* for 12 h. L-Mac (+MSCs transwell) indicates leukemic
741 macrophages, which were co-cultured in transwell with MSCs *in vitro* for 12 h. Y-axis indicates
742 the expression value. The expression value (DESeq2 normalized counts) of each gene is illustrated
743 by graphpad. Each column represents a replicate. **(G)** RNA-Seq analysis of *Arg1* in leukemic
744 macrophages sorted from MSC-treated leukemic mice *in vivo*. Leukemic macrophages
745 ($CD11b^{+}F4/80^{+}$) were sorted from the injected site (MSC-treated tibia) and non-injected site
746 (untreated femur) of leukemic mice 12 h post-treatment. Y-axis indicates the expression value.
747 The expression value (DESeq2 normalized counts) of each gene is illustrated by graphpad. Each
748 column represents a replicate. **(H)** Representative intracellular staining plots of Arg1 proteins in
749 MSC-reprogrammed leukemic macrophages (E-Mac, MSC-injected site) and leukemic
750 macrophages (L-Mac, Non-injected site) from MSC-treated leukemic mice analyzed by flow
751 cytometry. The ratios of $Arg1^{high}$ macrophage subpopulation are shown from L-Mac and E-Mac.
752 The bone marrow nucleated cells from leukemia-bearing mouse 12 h post-treatment were prepared
753 for intracellular flow cytometry staining of Arg1. Macrophages are identified as
754 $CD45^{+}CD11b^{+}F4/80^{+}$. **(I)** Statistical analysis of the ratios of $Arg1^{high}$ macrophage subpopulation

755 in L-Mac and E-Mac. Data are analyzed by unpaired student's t-test (two-tailed). **$p < 0.01$. Data

756 are represented as mean ± SD (n = 4 mice for each group).

757

Figure 6

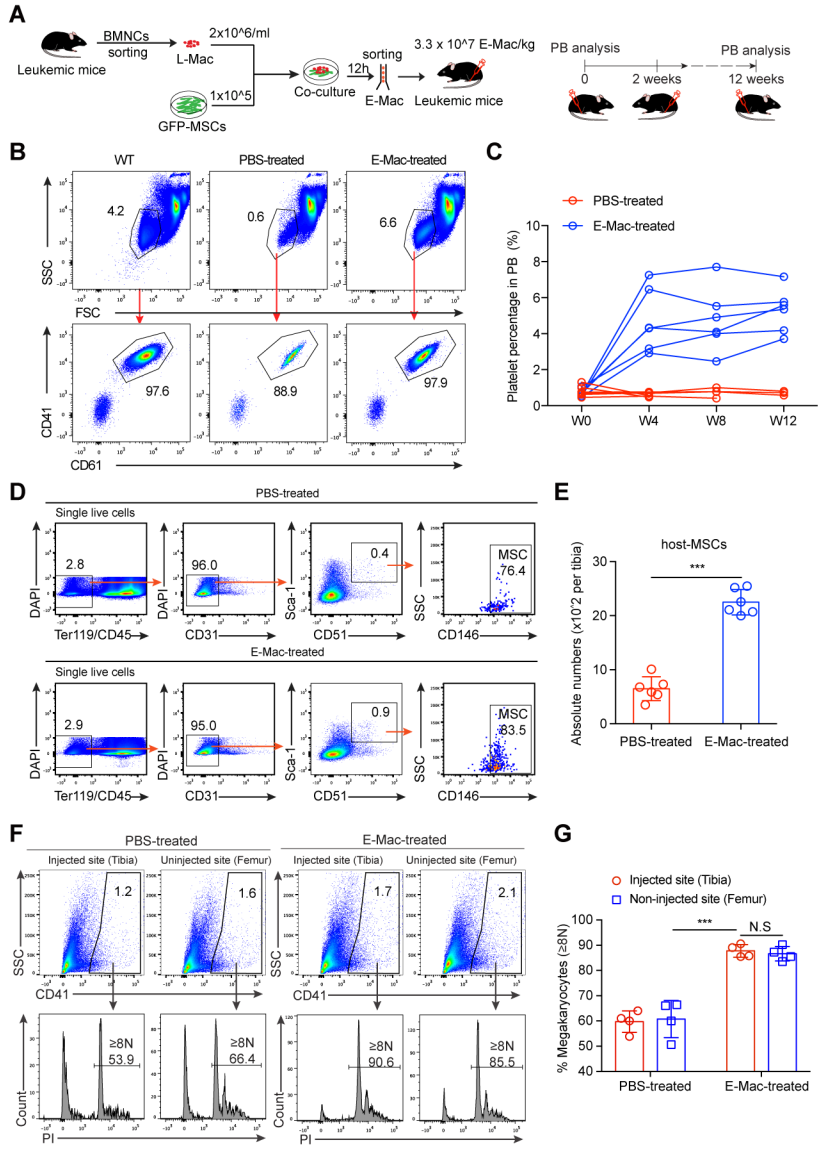

758

759 **Figure 6: Intra-bone-marrow transfusion of MSC-reprogrammed macrophages largely**

760 **rescues the therapeutic effects of MSC-treatment in leukemic mice**

761 **(A)** Schematic diagram of MSC-reprogrammed macrophages transfusion strategy. 1 × 10^5 GFP^+

762 MSCs were seeded into each well of six-well plates. $CD11b^+$ leukemic cells were enriched from

763 bone marrow of leukemic mice with severe tumor burden ($CD11b^+$% in PB > 60%). Then 2 × 10^6

764 $CD11b^+$ leukemic cells were directly co-cultured with MSCs. After 12 hours, leukemic

765 macrophages ($CD11b^+F4/80^+$) were sorted for transfusion. Leukemic mice with severe tumor

766 burden were treated by intra-bone-marrow transfusion of PBS or MSC-reprogrammed leukemic
767 macrophages (E-Mac). A sequential doses of E-Mac (3.3 × 10^7 E-Mac/kg per dose in 20 μl PBS)
768 were delivered into the tibia cavity using 29-gauge needle. Every tibia was treated once per two
769 weeks by switching the injection site every other dose. Analysis of platelets and $CD11b^+$ cells in
770 PB was performed monthly. **(B)** Representative dot plots of platelet populations and quantitative
771 gating, as identified by CD41 and CD61 staining in PB of WT mice and PBS/E-Mac treated
772 leukemic mice. After 4 weeks of PBS/E-Mac treatment, PB of leukemic mice with PBS/E-Mac
773 treatment was analyzed. **(C)** Kinetic analysis of platelets in PB of leukemia-bearing mice treated
774 with PBS or E-Mac (n = 6 mice for each group). **(D)** Flow cytometry analysis of MSCs in
775 leukemia-bearing mice post PBS/E-Mac treatment. Tibias of PBS/E-Mac treated leukemic mice at
776 week five since the first dose of PBS/E-Mac treatment were analyzed. MSCs were defined as
777 $Ter119^-CD45^-CD31^-Sca1^+CD51^+CD146^+$. The nucleated cell mixtures of BM and compact bones
778 were prepared for flow cytometry analysis of MSCs. **(E)** Statistical analysis of the absolute
779 numbers of host MSCs in tibias from PBS/E-Mac treated leukemic mice. Data are analyzed by
780 unpaired student's t-test (two-tailed). ***$p < 0.001$. Data are represented as mean ± SD (n = 6
781 mice for each group). **(F)** $CD41^+$ megakaryocytes from BM of PBS/E-Mac-injected site (tibia) and
782 non-injected site (femur) were analyzed for DNA content. Plots from representative PBS-treated
783 and E-Mac-treated leukemic mice four weeks post PBS/E-Mac treatment are shown. Percentages
784 of mature megakaryocytes with 8N and greater ploidy (≥8N) are shown. **(G)** Statistical analysis
785 of the percentages of mature megakaryocytes (≥8N) of $CD41^+$ BM megakaryocytes. Data are
786 analyzed by one-way ANOVA test. ***$p < 0.001$. Data are represented as mean ± SD (n = 4 mice
787 for each group).
788

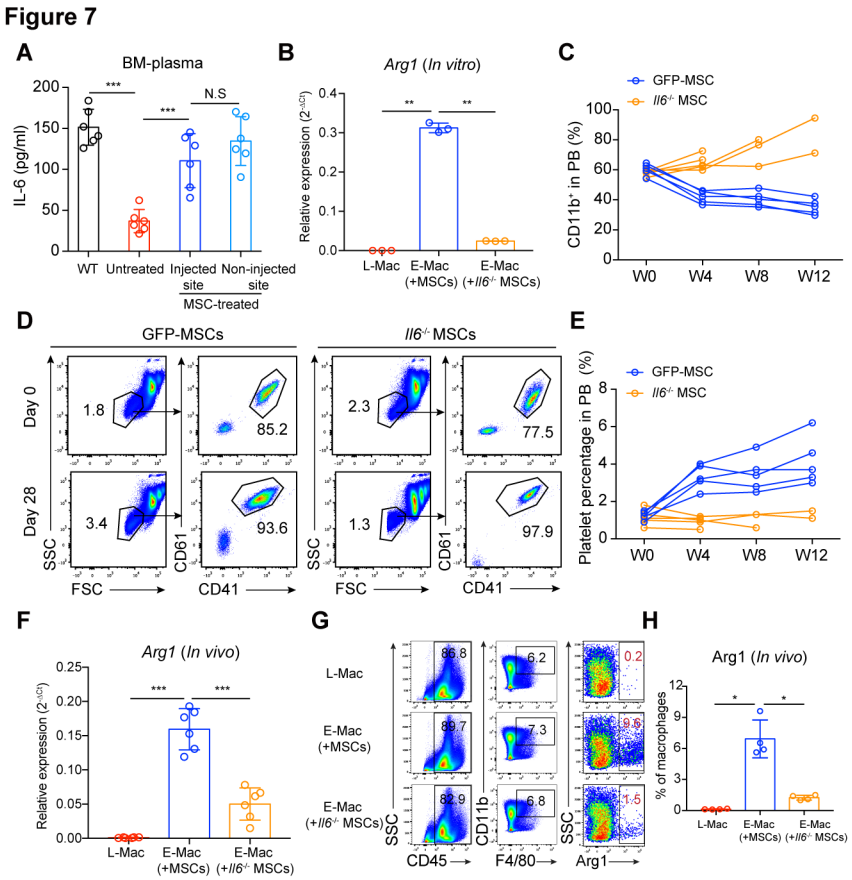

789

790 **Figure 7: *Il6*$^{-/-}$ MSCs neither reprogram macrophages nor suppress leukemia**

791 **(A)** ELISA of IL-6 levels in BM plasma. The BM plasma from WT mice, untreated leukemia-
792 bearing mice, and MSC-injected sites (tibias) and non-injected sites (femurs) of MSC-treated
793 leukemia-bearing mice eight weeks post MSC treatment were analyzed. The BMNC of each tibia
794 or femur were flushed out using 1 ml PBS, then the supernatants of each sample were collected
795 for ELISA. Data are analyzed by one-way ANOVA test. ***$p < 0.001$. Data are represented as
796 mean ± SD (n = 6 mice). **(B)** Q-PCR of *Arg1* expression levels in macrophages from leukemia-
797 bearing mice after co-culture with different sources of MSCs *in vitro*. Macrophages from
798 leukemia-bearing mice were co-cultured with MSCs from leukemia-bearing mice, *Il6*$^{-/-}$ MSCs or
799 GFP-MSCs *in vitro* for 12 h, separately. Then, one hundred thousand E-Mac ($CD11b^{+}F4/80^{+}$) were
800 sorted and were analyzed the expression of *Arg1*. Y-axis shows the relative expression of *Arg1* in

801 each group. Gapdh was used as a reference. Data are analyzed by one-way ANOVA test. **p <
802 0.01. Data are represented as mean ± SD (n = 3 repeats for each group). **(C)** Kinetic analysis of
803 tumor burden ($CD11b^+$) in PB of leukemia-bearing mice treated with GFP-MSCs or *Il6*$^{-/-}$ MSCs
804 (n = 5 mice for each group). **(D)** Flow cytometry analysis of platelets in *Il6*$^{-/-}$ MSC-treated
805 leukemia-bearing mice. Representative dot plots of platelet populations and quantitative gating, as
806 identified by CD41 and CD61 staining in PB of GFP-MSC- or *Il6*$^{-/-}$ MSC-treated leukemia-bearing
807 mice. PB of leukemia-bearing mice was analyzed at week-0 and week-4 post-treatment with GFP-
808 MSCs or *Il6*$^{-/-}$ MSCs. **(E)** Kinetic analysis of platelets (PLT) in PB of leukemia-bearing mice
809 treated with GFP-MSCs or *Il6*$^{-/-}$ MSCs (n = 5 mice for each group). **(F)** Q-PCR of *Arg1* expression
810 levels in macrophages isolated from *Il6*$^{-/-}$ MSC-treated leukemia-bearing mice. One hundred
811 thousand leukemic macrophages ($CD11b^+F4/80^+$) were sorted from the MSC-injected site (MSC-
812 treated tibia) and non-injected site (femur) of leukemia-bearing mice 12h post-treatment. Y-axis
813 shows the relative expression of *Arg1* in each group. Gapdh was used as reference. Data are
814 analyzed by one-way ANOVA test. ***p < 0.001. Data are represented as mean ± SD (n = 6 mice
815 for each group). **(G)** Representative intracellular staining plots of Arg1 proteins in MSC-
816 reprogrammed leukemic macrophages (E-Mac, MSC-injected sites) and leukemic macrophages
817 (L-Mac, Non-injected site) from GFP-MSC- or *Il6*$^{-/-}$ MSC-treated leukemic mouse analyzed by
818 flow cytometry. The ratios of $Arg1^{high}$ macrophage subpopulation are shown from L-Mac and E-
819 Mac. The bone marrow nucleated cells from leukemia-bearing mouse 12 h post-treatment were
820 prepared for intracellular flow cytometry staining of Arg1. Macrophages are identified as
821 $CD45^+CD11b^+F4/80^+$. **(H)** Statistical analysis of the ratios of $Arg1^{high}$ macrophage subpopulation.
822 Data are analyzed by one-way ANOVA test. *p < 0.05. Data are represented as mean ± SD (n = 4
823 mice for each group).